Simulations in Nonlinear Behavior of an Electrostatically-actuated Corrugated Diaphragm in Microelectromechanical System Tunable Filters

Yu-Chiao Wu, and Dimitrios Peroulis
Birck Nanotechnology Center, Purdue University, Indiana, United States of America

Summary. This study investigates the nonlinear behavior of a circular corrugated metallic diaphragm of a unique MEMS tuner in MEMS-tunable resonators that enables such characteristics from sub-GHz to over 100 GHz. In order to achieve a wide tunable frequency range, a large deflection of the diaphragm actuated by a given DC voltage is needed which results in a nonlinear behavior. In this simulation, the corrugated diaphragm was modeled as a membrane. The sidewalls of the corrugated rings were treated as a Belleville spring. During actuation, the stretch of the diaphragm produces an internal tension to enhance the stiffness of the diaphragm. However, the internal tension can also cause rotations of the sidewalls of the corrugated rings to decrease the induced internal tension. In this simulation, the finite difference method was used to numerically solve the governing nonlinear differential equation of a membrane. The rotation of each sidewall of the corrugated rings can be obtained analytically. Through the relationship among the radial displacements, the induced internal tension can be determined. The modeling results illustrate that the corrugated profile can reduce the internal tension. For a given maximum deflection, the internal tension decreases as the number of the corrugated rings is increased. In addition, a larger actuation voltage is needed for a corrugated diaphragm with a higher initial tension.

Introduction

MEMS-tunable resonators are highly desirable in high-frequency reconfigurable communication systems and radars due to their high quality factors and high tuning ratios [1, 2]. Several MEMS-tunable evanescent-mode resonators and filters which were made with MEMS tuners integrated with Si-based cavities have been recently reported [3, 4]. Frequency tuning in the order of an octave these demonstrations has been achieved by adjusting the small gap between the corrugated diaphragm and the post of the cavity.

This study investigates the nonlinear behavior of the corrugated circular diaphragm due to electrostatic actuation. With a given DC voltage, an electrostatic force is generated to pull the diaphragm towards the actuation electrode. Consequently, the gap between the diaphragm and the post of the cavity increases. In order to achieve a wide tuning range a large deflection of the diaphragm is required. The diaphragm, therefore, can be considered as a movable membrane. Since the depth of the corrugated rings is comparable to the thickness of the diaphragm, the deflection of the sidewalls of the corrugated rings due to bending can be neglected. Hence, each sidewall was modeled as a Belleville spring. During actuation, internal tension is induced due to stretching of the diaphragm. This induced tension causes the sidewalls of the corrugated rings to rotate. The rotations produce radial displacements and further decrease the internal tension. This study focuses on modeling electrostatically-actuated corrugated membranes with different numbers of corrugated rings and with different initial tensions.

Simulation Theory

A schematic of a typical corrugated circular diaphragm is shown in Fig. 1. It is noted that all regions $H \cot \varphi$ of corrugated rings are much smaller than any interval between R_i and R_{i+1}, i.e. $H \cot \varphi \ll R_i - R_{i+1}$. As the electrostatically-actuated diaphragm is treated as a membrane, the governing equation is given by:

$$\frac{\partial^2 z}{\partial r^2} + \frac{1}{r}\frac{\partial z}{\partial r} = -\frac{\epsilon_0 \alpha}{2(g_0 - z)^2} \tag{1}$$

where ϵ_0 is free-space permittivity, V is the DC voltage, g_0 is the gap between the diaphragm and the electrode, and $\alpha = V^2/N$ in which V is the DC voltage, and N is the internal tension.

As the sidewalls are simulated as a Belleville spring, the rotation of a Belleville spring is obtained as: $2NR_i/EhH$ [5] where E and h are the Young's modulus and thickness of the diaphragm. Through the displacement relationship, i.e. $2\int_0^{R_0} d(ur) \approx \int_0^{R_0} (\partial z/\partial r)^2 r\, dr$ [6], the internal tension N can be determined by:

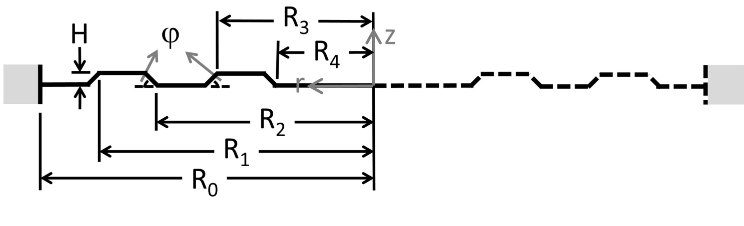

Figure 1: Sketch of a corrugated circular diaphragm.

$$\frac{NR_0^2\left(1-\nu^2\right)}{Eh}+\sum_{i=1}^{n}\frac{2NR_i^2}{Eh}=\frac{1}{2}\int_0^{R_0}\left(\frac{\partial z}{\partial r}\right)^2 r\,dr \tag{2}$$

where ν is Poisson's ratio, and n is the number of R_i.
The finite difference method is used to solve Eqs. (1) and (2). The computation procedure starts by providing a value to α first [7, 8]. Then the deflection z of the diaphragm is obtained by solving Eq. (1). Consequently, the internal tension N can be determined by Eq. (2). The DC voltage V is found via $V=\sqrt{\alpha N}$.

Discussion

In this simulation, the diaphragm is assumed to be made of gold, i.e. $E = 79$ GPa and $\nu = 0.44$, and with $R_0 = 2$ mm, $h = 2\ \mu m$, $H = 5\ \mu m$, $\varphi = \pi/4$, and $g_0 = 70\ \mu m$. Figure 2 shows the maximum deflection versus the DC voltage for diaphragms with different number of corrugated rings. It can be found that the required DC voltage is significantly reduced for a corrugated diaphragm. A diaphragm with fewer corrugated rings needs higher DC voltage to be actuated. Figure 3 illustrates the maximum deflection versus the DC voltage for diaphragms with different initial tension, i.e. N_i =0, 0.1, 0.5 N/m. A diaphragm with higher initial tension needs a higher DC voltage to be actuated.

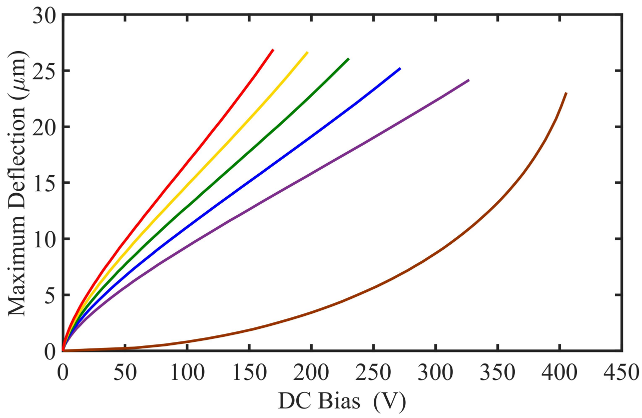

Figure 2: Maximum deflection vs. DC voltage for diaphragms with $R_0 = 2$ mm and different numbers of corrugated rings: the brown line is for a flat diaphragm; the purple line represents $R_i = 1$ and 1.1 mm; the blue line illustrates $R_i = 1$, 1.1, 1.2, and 1.3 mm; the green line shows $R_i = 1$, 1.1, 1.2, 1.3, 1.4, and 1.5 mm; the yellow line represents $R_i = 1$, 1.1, 1.2, 1.3, 1.4, 1.5, 1.6, and 1.7 mm, and the red line illustrates $R_i = 1$, 1.1, 1.2, 1.3, 1.4, 1.5, 1.6, 1.7, 1.8, and 1.9 mm.

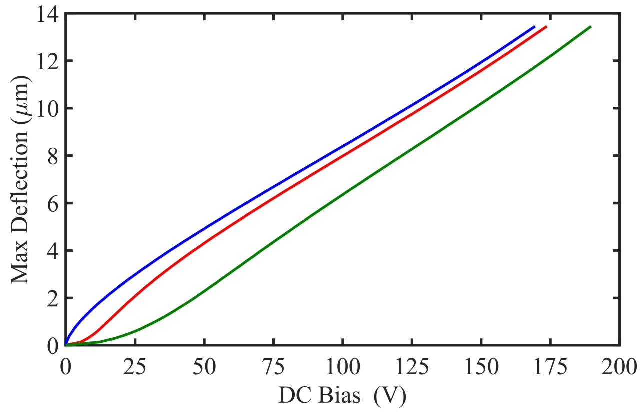

Figure 3: Maximum deflection vs. DC voltage for diaphragms with $R_0 = 2$ mm and $R_i = 1$, 1.1, 1.2, 1.3, 1.4, 1.5, 1.6, 1.7, 1.8, and 1.9 mm and different initial tensions (N_i): the blue line shows $N_i = 0$ N/m; the red line represents $N_i = 0.1$ N/m, and the green line illustrates $N_i = 0.5$ N/m.

Conclusions

The nonlinear behavior of an electrostatically-actuated corrugated circular diaphragm has been numerically investigated. The finite difference method was applied to solve the nonlinear differential equation for the diaphragm. The results show that the applied DC voltage is decreased as the number of corrugated rings is increased. In addition, a relatively large DC voltage is required for a corrugated diaphragm with high initial tension.

References

[1] Liu, Xiaoguang and Katehi, Linda PB and Chappell, William J and Peroulis, Dimitrios (2010) High-tunable microwave cavity resonators and filters using SOI-based RF MEMS tuners *J. Microelectromechanical Sys* **19**:774-784.

[2] Arif, Muhammad Shoaib and Peroulis, Dimitrios (2012) A 6 to 24 GHz continuously tunable, microfabricated, high-Q cavity resonator with electrostatic MEMS actuation *2012 IEEE MTT-S Int. Microwave Symp. (IMS2012)* 1-3.

[3] Yang, ZhengAn and Peroulis, Dimitrios (2014) A 23–35 GHz MEMS tunable all-silicon cavity filter with stability characterization up to 140 million cycles *2014 IEEE MTT-S Int. Microwave Symp. (IMS2014)* 1-4.

[4] Hickle, Mark D and Sinanis, Michael D and Peroulis, Dimitrios (2016) Design and implementation of an intrinsically-switched 22–43 GHz tunable bandstop filter *2016 IEEE 17th Annual Wireless and Microwave Tech. Conf. (WAMICON)* 1-3.

[5] Timoshenko S. (1930) Strength of materials. D. Van Nostrand Company, NY.

[6] Williams, J (1997) Energy release rates for the peeling of flexible membranes and the analysis of blister tests *Int. J. Fracture* **87**:265-288.

[7] Yang, F. (2002) Electromechanical instability of microscale structures *J. appl. phys.* **92**:2789-2794.

[8] Wu, Y.-C. and Adams, G. (2009) A robust analysis of the actuation of a carbon-nanotube-based nanoswitch with sidewall slip *J. appl. phys.* **106**:054310.